

Electron-impact excitation of the $B^1\Sigma_u^+$ and $C^1\Pi_u$ electronic states of H_2

H. Kato, H. Kawahara, M. Hoshino, and H. Tanaka
Physics Department, Sophia University, Chiyoda-ku, Tokyo 102-8554, Japan

L. Campbell and M. J. Brunger*
ARC Centre for Antimatter-Matter Studies, SoCPES, Flinders University, G.P.O. Box 2100, Adelaide SA 5001, Australia
 (Received 14 April 2008; published 16 June 2008)

Differential and integral cross sections for electron-impact excitation of the dipole-allowed $B^1\Sigma_u^+$ and $C^1\Pi_u$ electronic states of molecular hydrogen have been measured. The differential cross sections were determined by analysis of normalized energy-loss spectra obtained using a crossed-beam apparatus at the electron-impact energies of 40, 100, and 200 eV. Integral cross sections were subsequently derived from these data. The present work was undertaken in order to investigate some ambiguities between earlier experimental data and recent BEf-scaled cross sections as defined and calculated by Kim [J. Chem. Phys. **126**, 064305 (2007)] and also to extend the energy range of the available data. Optical oscillator strengths, also determined as a part of the present investigation, were found to be in fair accordance with previous measurements and some calculations.

DOI: [10.1103/PhysRevA.77.062708](https://doi.org/10.1103/PhysRevA.77.062708)

PACS number(s): 34.80.Gs

I. INTRODUCTION

Electron-impact collision cross sections of H_2 are crucial input data for the modeling of fusion plasmas and in astrophysics. They also in principle play an important role in the development of collision theory for electron-molecule interactions, because H_2 is the simplest neutral molecule and very accurate wave functions are already available for its low-lying electronic states [1]. It is therefore a little surprising that the results from only three differential cross-section (DCS) measurements, for the $B^1\Sigma_u^+$ and $C^1\Pi_u$ electronic states, have thus far been published in the literature with, arguably, each of them originating from the same group [2–4]. The situation is even worse from a theoretical perspective, where DCS computations from Fliflet and McKoy [5] using a distorted-wave approach and Gibson *et al.* [6] using a Schwinger multichannel calculation, for the $B^1\Sigma_u^+$ state and over a quite restricted energy range, appear to be the only results in the literature. At the integral cross-section (ICS) level we have experimental results derived from the DCS data [2–4], as well as optical measurements for both states from Ajello *et al.* [7]. With regard to theory for the ICS, we find that the situation is much improved. In addition to results from Fliflet and McKoy [5] and Gibson *et al.* [6], we note impact-parameter method computations for both states [8,9], plane-wave Born results [10], B - and C -state R -matrix computations [11], and results for both states from Kim [1] produced using the BE- and BEf-scalings defined in that paper. Indeed it is the work of Kim, who highlighted ambiguities between his BEf-scaled integral cross sections and the existing measurements, in particular for the C state, that motivated, in part, the present study. An additional motivation for our work was that previously all measurements were restricted to energies less than 60 eV, while here we extend the impact-energy range up to 200 eV.

Contrary to the story outlined above, with respect to measurements and calculations for the optical oscillator strengths

of the $B^1\Sigma_u^+$ and $C^1\Pi_u$ states, we find that there has been significant work undertaken. This work is summarized in Kim [1] and references therein, with some of the most important experimental studies being due to Chan *et al.* [12], Xu *et al.* [13], Geiger and Schmoranzner [14], and Fabian and Lewis [15]. Corresponding theory work is from Allison and Dalgarno [16,17], Liu and Hagstrom [18], Borges and Bielschowsky [19], and Arrighini *et al.* [10]. Recall that the optical oscillator strengths represent a very sensitive test for the validity of the structure representation in a calculation, and as such, they are important physical quantities. For completeness, we also note the detailed summary of optical oscillator strengths from Berkowitz [20].

In the next section we describe our experimental measurements and our spectral deconvolution of the energy-loss spectra in order to extract the DCS. This is followed by a description, in Sec. III, of both our generalized oscillator strength (GOS) analysis of the measured DCS and how our integral cross sections are derived. In Sec. IV our results are presented and discussed, with some conclusions from the current investigation being given in Sec. V.

II. EXPERIMENTAL DETAILS AND SPECTRAL DECONVOLUTION TECHNIQUES

The present spectrometer [21] consists of an electron gun with a hemispherical monochromator, a molecular hydrogen beam crossed at right angles to the incident electrons, and a rotatable detector ($\theta_e = -10^\circ - 130^\circ$) with a second hemispherical analyzer system. A number of electron optic elements (tube symmetry) image and energy-control the electron beam, with their performance having been rigorously checked by electron trajectory calculations. Both the monochromator and the analyzer are enclosed in differentially pumped boxes in order to reduce the effect of any background gases and to minimize the stray electron background. The target molecular beam is produced by effusing H_2 through a simple nozzle with an internal diameter of 0.3 mm and a length of 5 mm. The spectrometer and the nozzle are

*Michael.Brunger@flinders.edu.au

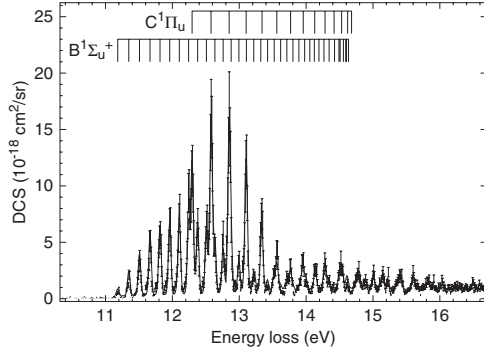


FIG. 1. Typical energy-loss spectrum and spectral deconvolution for 40 eV, 10° . The present data (\circ) and our fit to those data (solid line) are shown. Also plotted are the relevant vibrational sublevels of the respective $B^1\Sigma_u^+$ and $C^1\Pi_u$ electronic states.

both heated to a temperature of $\approx 50^\circ\text{C}$ to minimize any possible contamination during the measurements. The current energy range is $E_0=40\text{--}200$ eV, and the scattered electron angular range is $4.1^\circ\text{--}30.0^\circ$. In all of these cases the energy resolution was 30–35 meV [full width at half maximum (FWHM)] and the angular resolution was $\sim \pm 1.5^\circ$ (FWHM). The primary electron beam current was in the range of 3–9 nA. Furthermore, the voltages for both the input and output lenses of the hemispheres were carefully adjusted to ensure that the base resolution of the energy-loss spectra remained as symmetric as possible.

Energy-loss spectra were measured, at each incident electron energy and each scattered electron angle, over the energy-loss range encompassing the elastic peak and from ~ 10.3 to 16.7 eV. A typical example of these data at $E_0=40$ eV and $\theta_e=10^\circ$ is shown in Fig. 1, where we note that the elastic peak has been suppressed for the sake of clarity. The absolute scales (see the y axis) of the present energy-loss spectra were set using the relative flow technique [22] with helium elastic DCSs as the standard [23]. In addition, at 100 and 200 eV, this normalization was cross-checked using the known helium 2^1P inelastic DCSs [24]. Consistent results were obtained in each case. For the incident energies of interest ($E_0=40, 100,$ and 200 eV) and the energy-loss range of interest ($\Delta E \approx 0\text{--}16.7$ eV), the ratio of the energy loss to the incident energy varies roughly in the range of $0 \leq \Delta E/E_0 < 0.42$. Thus it is important to establish the transmission of the analyzer over this energy-loss range, with our procedure for doing so being found in Kato *et al.* [25].

The final complication in the present study is that there are many overlapping vibrational sublevels of the respective H_2 electronic states in the ~ 10.3 to 16.7 eV energy-loss range. As a consequence, the various $B^1\Sigma_u^+$ and $C^1\Pi_u$ contributions to the energy-loss spectra had to be spectrally deconvolved. To this end we adapted the approach outlined in detail in Campbell *et al.* [26], modified here to incorporate the relevant energies and Franck-Condon factors from Wrkich *et al.* [4] and from the International Atomic Energy Agency (IAEA) website [27]. A representative example of the quality of the present spectral fits to our measured energy-loss data is given in Fig. 1 (solid line), where we see that the quality of the fit is excellent. Note that in Fig. 1 we

also plot the vibrational sublevels of both the $B^1\Sigma_u^+$ and $C^1\Pi_u$ electronic states. This was done in order to give the reader an appreciation of the difficulty of that task, although we believe that our procedure gives unique B - and C -state manifold differential cross sections to within our stated uncertainties. The present $B^1\Sigma_u^+$ and $C^1\Pi_u$ DCSs are plotted in Fig. 2(a) [(i)–(iii)] and Fig. 2(b) [(i)–(iii)], respectively. They are also tabulated in Tables I and II, with our estimated errors on these data being in the range 18–20 %, which includes an allowance for the uncertainty in our spectral deconvolution and our normalization.

III. ANALYSIS DETAILS

The values of $[\theta_e, \mathcal{D}\sigma(\theta_e)]$ from the present study, for each electronic state at each incident electron energy, are transformed to (K^2, G_{expt}) using the standard formula [1]

$$G_{\text{expt}}(K^2) = \frac{(E/R)k_i a_0}{4a_0^2 k_f a_0} K^2 \mathcal{D}\sigma(E_0, \theta_e), \quad (1)$$

where k_i and k_f are the initial and final momenta of the incident electron, E is the excitation energy for each electronic state, a_0 is the Bohr radius (0.529 Å), R is the Rydberg energy (13.6 eV), θ_e is the electron scattering angle, $G_{\text{expt}}(K^2)$ is the experimental generalized oscillator strength, $\mathcal{D}\sigma$ is the DCS, and K^2 is the momentum transfer squared defined by

$$K^2 = (k_i a_0)^2 + (k_f a_0)^2 - 2(k_i a_0)(k_f a_0) \cos \theta. \quad (2)$$

Vriens [28] proposed the following formula to represent the generalized oscillator strength for a dipole-allowed excitation based on the analytic properties identified by Lassette [29] and Rau and Fano [30]:

$$G(X) = \frac{1}{(1+X)^6} \left[\sum_{m=0}^{\infty} \frac{f_m X^m}{(1+X)^m} \right], \quad (3)$$

where

$$X = \frac{K^2}{\alpha^2} \quad (4)$$

and

$$\alpha = \sqrt{B/R} + \sqrt{(B-E)/R}. \quad (5)$$

Note that, in Eq. (5), B is the binding energy of the target electron.

In Eq. (3) the f_m are fitting constants to be determined in a least-squares fit analysis of the experimental generalized oscillator strengths, which we reiterate are calculated from the DCSs of the study. Examples of the quality of those fits, for both the $B^1\Sigma_u^+$ and $C^1\Pi_u$ states, are given in Fig. 3. The beauty of Vriens' [28] formalism is that at the $X=0$ optical limit, the value of $G(0) \equiv f_0$ is the optical oscillator strength (OOS). The present OOSs, as derived from an analysis of our 100-eV and 200-eV data, are given in Table III. Also listed in Table III are the OOSs for the $B^1\Sigma_u^+$ and $C^1\Pi_u$ electronic states from previous measurements [12–15] and calculations [10,16–19].

Finally, estimates of the ICS (σ) at each energy can be obtained from Eqs. (3)–(5) using the standard formulas [31]

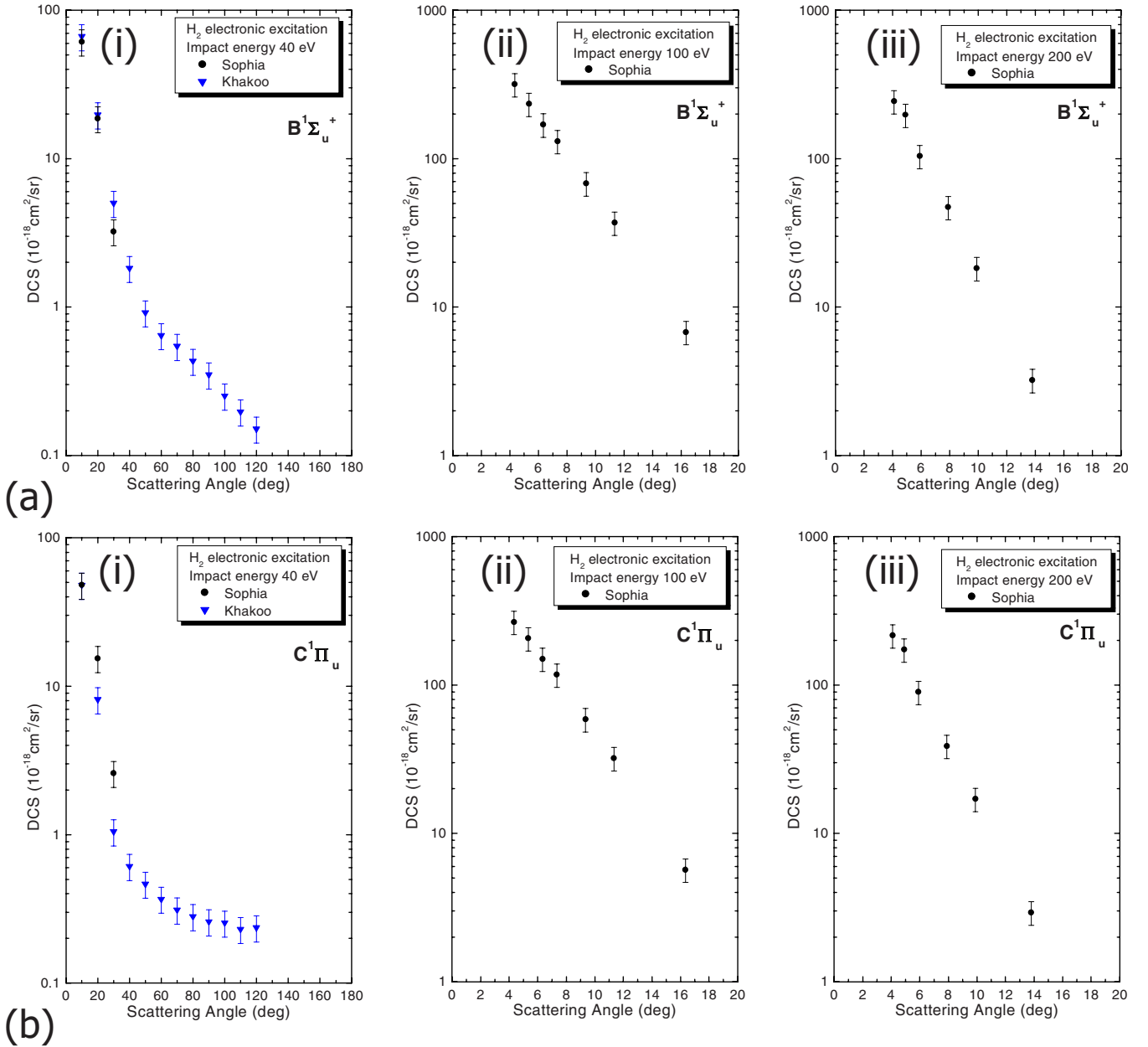


FIG. 2. (Color online) DCS (10^{-18} cm²/sr) at (i) 40, (ii) 100, and (iii) 200 eV for the (a) $B^1\Sigma_u^+$ and (b) $C^1\Pi_u$ electronic states. The present data (●) and the earlier data of Khakoo and Trajmar (▼) are shown.

$$\sigma(E_0) = \frac{4\pi a_0^2}{E_0/R} \int_{K_{\min}^2}^{K_{\max}^2} \frac{G(K^2)}{E/R} d \ln(K^2), \quad (6)$$

with

$$K_{\min}^2 = 2 \frac{E_0}{R} \left[1 - \frac{E}{2E_0} - \sqrt{1 - E/E_0} \right] \quad (7)$$

and

$$K_{\max}^2 = 2 \frac{E_0}{R} \left[1 - \frac{E}{2E_0} + \sqrt{1 - E/E_0} \right]. \quad (8)$$

The results from this latter process are listed in Tables IV and V and plotted in Figs. 4(a) and 4(b).

IV. RESULTS AND DISCUSSION

In Fig. 2 and Tables I and II, we present our differential cross sections for the electron-impact excitation of the respective $B^1\Sigma_u^+$ and $C^1\Pi_u$ electronic states in H₂. Also included in Fig. 2, where appropriate, are the corresponding earlier results from Khakoo and Trajmar [3]. It is clear from this figure that both the present B - and C -state DCSs are strongly peaked in magnitude, as one goes to the more forward scattering angles. This result is consistent with the fact that in each case the excitation process is dipole allowed. If we now compare the present 40-eV $B^1\Sigma_u^+$ DCSs—see Fig. 2(a) [(i)]—to those from Khakoo and Trajmar [3], we find excellent agreement between them across the common angular range of measurement. This level of agreement does not,

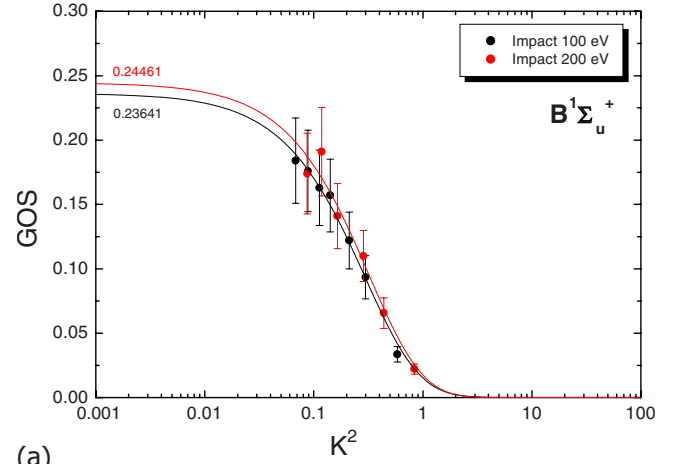
TABLE I. Present differential cross sections (10^{-18} cm²/sr) for electron-impact excitation of the $B^1\Sigma_u^+$ electronic state in H₂. The numbers in parentheses represent the percentage uncertainty in the DCSs.

θ_e°	Electron energy (eV)		
	40	100	200
4.1			244.04 (18%)
4.34		317.89 (18%)	
4.9			197.16 (18%)
5.34		234.19 (18%)	
5.9			104.10 (18%)
6.34		169.79 (18%)	
7.34		131.15 (18%)	
7.9			47.08 (18%)
9.34		68.17 (18%)	
9.9			18.27 (18%)
10	61.43 (20%)		
11.34		37.02 (18%)	
13.8			3.22 (18%)
16.34		6.78 (18%)	
20	18.68 (20%)		
30	3.23 (20%)		

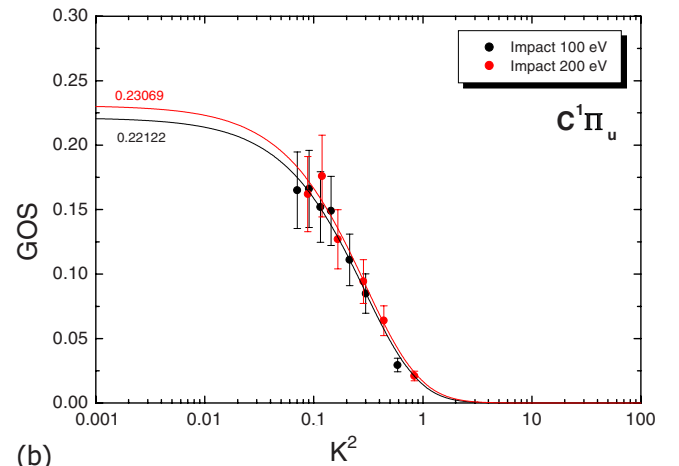
however, extend to the $C^1\Pi_u$ state—see Fig. 2(b) [(i)]—where the present DCSs are systematically higher in magnitude (by a factor of ≈ 2) compared to those from Khakoo and Trajmar. This is an important result because as the ICSs are derived from the DCSs, and as most of the contribution to

TABLE II. Present differential cross sections (10^{-18} cm²/sr) for electron-impact excitation of the $C^1\Pi_u$ electronic state in H₂. The numbers in parentheses represent the percentage uncertainty in the DCSs.

θ_e°	Electron energy (eV)		
	40	100	200
4.1			216.11 (18%)
4.34		266.10 (18%)	
4.9			173.76(18%)
5.34		206.95 (18%)	
5.9			89.84 (18%)
6.34		149.96 (18%)	
7.34		117.62 (18%)	
7.9			38.80 (18%)
9.34		58.79 (18%)	
9.9			17.07 (18%)
10	48.09 (20%)		
11.34		32.12 (18%)	
13.8			2.93 (18%)
16.34		5.69 (18%)	
20	15.44 (20%)		
30	2.60 (20%)		



(a)



(b)

FIG. 3. (Color online) Present GOS versus K^2 plots at 100 eV (black solid circles) and 200 eV (red solid circles) for the (a) $B^1\Sigma_u^+$ and (b) $C^1\Pi_u$ electronic states. The fits to the data were performed using the formalism outlined in Sec. III of the paper.

the ICSs in this case will come from the more forward scattering angles, the present $C^1\Pi_u$ ICS at 40 eV must be significantly higher in magnitude than that reported previously by Khakoo and Trajmar. We will come back to this point shortly.

Following the methodology outlined in Sec. III, the measured DCSs at 100 eV and 200 eV and for both states were, respectively, converted into GOS as a function of K^2 . Those data and the results of least-squares fits using the form of Eqs. (3)–(5) are plotted in Figs. 3(a) and 3(b). In each case the fits to the 100-eV and 200-eV data are seen to be almost identical, with the corresponding derived optical oscillator strengths being equivalent to within the respective uncertainties. Indeed a single function could be easily fitted to a combined 100-eV and 200-eV data set, which is a necessary prerequisite for the validity of this approach in determining OOSs. The present $B^1\Sigma_u^+$ and $C^1\Pi_u$ OOSs are given in Table III, along with earlier experimental [12–15,20] and theoretical [10,16–19] determinations. The present $B^1\Sigma_u^+$ optical oscillator strength, allowing for our uncertainty of $\sim 20\%$, is in very good agreement with the previous mea-

TABLE III. A comparison between the present optical oscillator strengths and a selection of those from previous workers [10,12–20]. The error in the present OOS is $\sim 20\%$.

	$C \ ^1\Pi_u$	$B \ ^1\Sigma_u^+$
Experiment		
Present work	0.226	0.241
Chan <i>et al.</i> [12]	0.322	0.301
Xu <i>et al.</i> [13]	0.321	0.280
Geiger and Schmoranzler [14]	0.263	0.287
Berkowitz [20]	0.356	0.311
Fabian and Lewis [15]	0.239	0.125
Theory		
Allison and Dalgarno [16,17]	0.357	0.311
Liu and Hagstrom [18]		0.321
Borges and Bielschowsky [19]	0.351	0.274
Arrighini <i>et al.</i> [10]	0.349	

surements, the only exception being that from Fabian and Lewis [15], which is about a factor of 2 smaller. Similarly our $B \ ^1\Sigma_u^+$ OOS agrees well with the results from theory [16–19], in particular with the most recent computation from Borges and Bielschowsky [19] (see Table III). On the other hand, our $C \ ^1\Pi_u$ OOS is in best agreement with the earlier experiments of Geiger and Schmoranzler [14] and Fabian and Lewis [15], all being somewhat lower in value compared to the more recent results of Chan *et al.* [12] and Xu *et al.* [13]. Nonetheless, even here, to within the various stated uncertainties, the level of agreement is satisfactory. Similar remarks to those just made for the experimental comparison are also applicable when the present $C \ ^1\Pi_u$ OOS is compared to results from available theory [10,16,17,19].

With respect to our ICSs, the present data are tabulated in Tables IV and V, along with previous results from Wrkich *et al.*

TABLE IV. Present experimental integral cross sections (10^{-16} cm^2) for electron-impact excitation of the $B \ ^1\Sigma_u^+$ electronic state in H_2 . The uncertainties in the present ICSs are $\sim 25\%$. Also shown are the earlier results from Wrkich *et al.* [4], Khakoo and Trajmar [3], and Srivastava and Jensen [2].

Energy (eV)	Present	ICS (10^{-16} cm^2)		
		Wrkich <i>et al.</i> [4]	Khakoo and Trajmar [3]	Srivastava and Jensen [2]
15				0.170
17.5		0.170		
20		0.277	0.212	0.250
30		0.318	0.244	0.240
40	0.276		0.304	0.280
50				0.240
60			0.295	0.180
100	0.246			
200	0.176			

TABLE V. Present experimental integral cross sections (10^{-16} cm^2) for electron-impact excitation of the $C \ ^1\Pi_u$ electronic state in H_2 . The uncertainties in the present ICSs are $\sim 25\%$. Also shown are the earlier results from Wrkich *et al.* [4] and Khakoo and Trajmar [3].

Energy (eV)	Present	ICS (10^{-16} cm^2)	
		Wrkich <i>et al.</i> [4]	Khakoo and Trajmar [3]
15			
17.5		0.088	
20		0.198	0.156
30		0.256	0.176
40	0.231		0.196
50			
60			0.222
100	0.212		
200	0.153		

al. [4], Khakoo and Trajmar [3], and Srivastava and Jensen [2]. These data are also plotted in Fig. 4(a) for the $B \ ^1\Sigma_u^+$ state and in Fig. 4(b) for the $C \ ^1\Pi_u$ state, along with calculated results from an impact-parameter theory approach [8,9], a seven-state R -matrix computation [11], a distorted-wave Born approximation [5], plane-wave (PW) Born and BE f -scaled techniques [1], and a Landolt-Börnstein compilation from Brunger *et al.* [32]. Also included in these plots are the emission data from Ajello *et al.* [7]. Considering first Fig. 4(a), the present data are seen to be in reasonable agreement with the results from Khakoo and Trajmar [3], as expected from the DCSs, and are consistent with the trend in the low-energy data from Wrkich *et al.* [4]. The higher-energy data from Srivastava and Jensen [2] appear to be too low in magnitude, while the emission result from Ajello *et al.* significantly overestimates the magnitude of the ICS (approximately a factor of 2) at 100 eV. This is likely to be due to cascade effects in their measurement. With respect to the available theories, the PW-Born [1], impact-parameter theory [8,9], R -matrix [11], and distorted-wave results [5] all significantly overestimate the magnitude of the ICS for electron-impact excitation of the $B \ ^1\Sigma_u^+$ state. Only the BE f -scaling result [1] is consistent with the data over the common energy range (from approximately equal to the threshold value to 200 eV), although the Landolt-Börnstein compilation [32] is also reasonable in this case. For the $C \ ^1\Pi_u$ electronic state, best agreement is again seen between the BE f -scaling result of Kim, the present data, and the earlier measurements from Wrkich *et al.* This observation, also consistent with what one previously observed at the DCS level for this state at 40 eV, confirms that the 30–60-eV ICSs of Khakoo and Trajmar are somewhat too low in magnitude. This therefore resolves the ambiguity originally noted by Kim [1], who had not expected the BE f -scaling result to fail at those energies, and indeed it does not. Similar to that described above for the $B \ ^1\Sigma_u^+$ state, here we also note [see Fig. 4(b)] that all the other computations [5,8,9,11] overestimate the magnitude of the $C \ ^1\Pi_u$ ICS, as does the emission measurement from Ajello *et al.* [7].

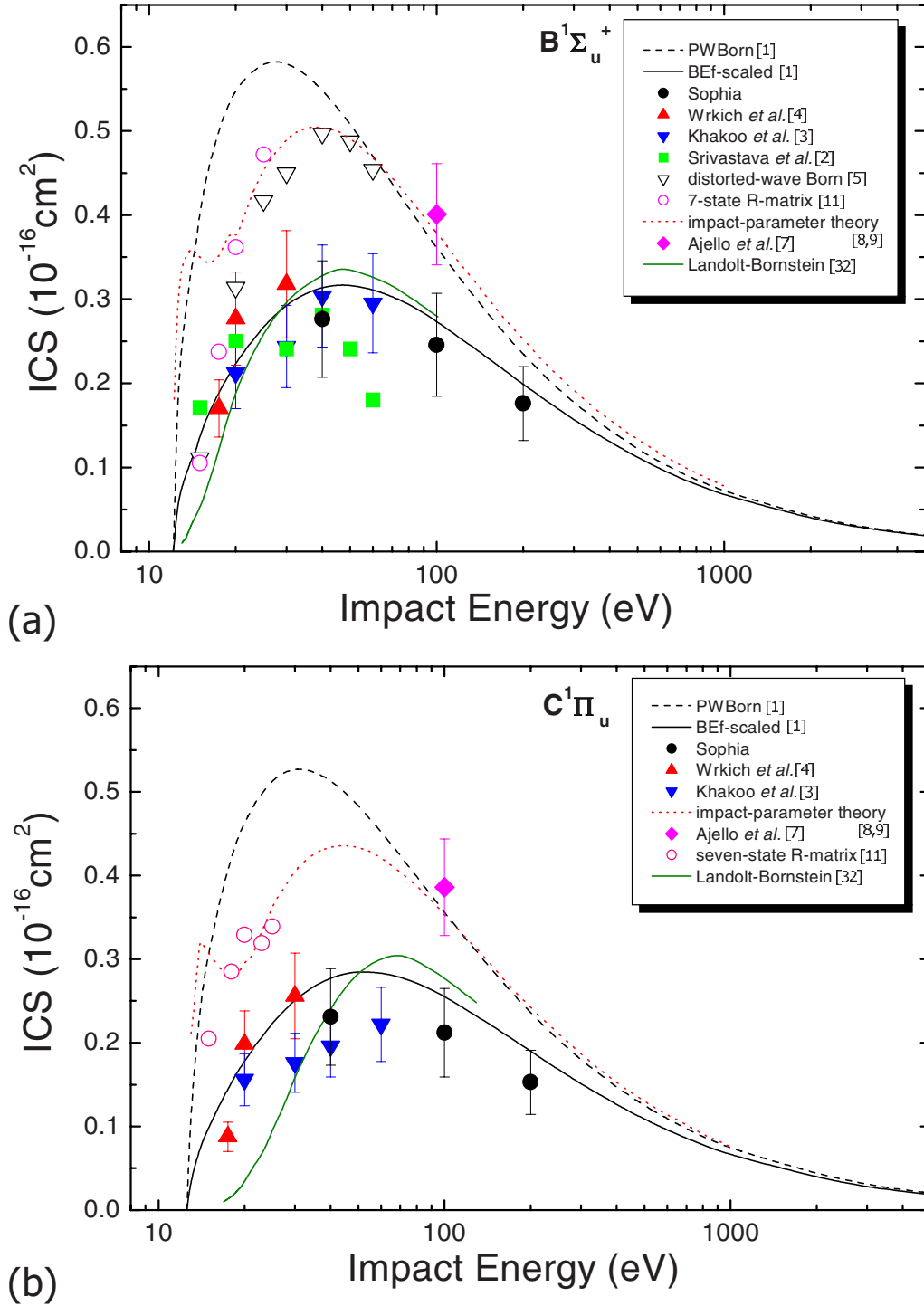


FIG. 4. (Color online) ICS (10^{-16} cm^2) plots for the (a) $B^1\Sigma_u^+$ and (b) $C^1\Pi_u$ electronic states. See legends in the figures for further details.

The present measurements, when combined with our previous work on H_2O [33], CO [25,34], and CO_2 [35], provide further strong evidence for the efficacy of the BEf-scaling approach in calculating ICSs for dipole-allowed excitations. We assert that any modeler studying applied phenomena, such as lighting or atmospheric behavior, and wishing to incorporate reliable atomic and molecular cross sections over extended energy ranges in their database, should give serious

consideration to utilizing the BEf-scaling approach of Kim [1].

V. CONCLUSIONS

We have reported manifold differential cross sections for electron-impact excitation of the $B^1\Sigma_u^+$ and $C^1\Pi_u$ electronic states in H_2 . At 40 eV good agreement was found between

the present data and that of Khakoo and Trajmar [3] for the $B \ ^1\Sigma_u^+$ state; however, for the $C \ ^1\Pi_u$ case the earlier DCS data [3] appear to have significantly underestimated the strength of its forward angle behavior. Optical oscillator strengths, derived from our analysis of the measured DCSs at 100 eV and 200 eV, were found to be in best agreement with those from Geiger and Schmoranzler [14]. However, most of the measured data [12–14], to within their experimental uncertainties, were in fact in fair accordance so that the OOSs for the respective B and C states can be considered to be well known. The present ICSs, when combined with the lower-energy results from Wrkich *et al.* [4], support the validity of the BEf-scaling results from Kim [1], for the B and C states,

over the common energy range. This observation therefore removes the ambiguity, first reported for the C state by Kim [1], that the higher-energy data of Khakoo and Trajmar [3] suggested that the BEf-scaling C -state results were in significant error.

ACKNOWLEDGMENTS

This work was supported by the Japanese Ministry of Education, Sports, Culture and Technology, Flinders University, and the Australian Research Council. We are grateful to Professor M. Khakoo for his suggestion that the H_2 system needed further measurements.

-
- [1] Y.-K. Kim, *J. Chem. Phys.* **126**, 064305 (2007).
 [2] S. K. Srivastava and S. Jensen, *J. Phys. B* **10**, 3341 (1977).
 [3] M. A. Khakoo and S. Trajmar, *Phys. Rev. A* **34**, 146 (1986).
 [4] J. Wrkich, D. Mathews, I. Kanik, S. Trajmar, and M. A. Khakoo, *J. Phys. B* **35**, 4695 (2002).
 [5] A. W. Fliflet and V. McKoy, *Phys. Rev. A* **21**, 1863 (1980).
 [6] T. L. Gibson, M. A. P. Lima, V. McKoy, and W. M. Huo, *Phys. Rev. A* **35**, 2473 (1987).
 [7] J. M. Ajello, D. Shemansky, T. L. Kwok, and Y. L. Yung, *Phys. Rev. A* **29**, 636 (1984).
 [8] M. J. Redmon, B. C. Garrett, L. T. Redmon, and C. W. McCurdy, *Phys. Rev. A* **32**, 3354 (1985).
 [9] R. Celiberto and T. N. Rescigno, *Phys. Rev. A* **47**, 1939 (1993).
 [10] G. P. Arrighini, F. Biondi, and C. Giudotti, *Mol. Phys.* **41**, 1501 (1980).
 [11] S. E. Branchett, J. Tennyson, and L. A. Morgan, *J. Phys. B* **23**, 4625 (1990).
 [12] W. F. Chan, G. Cooper, and C. E. Brion, *Chem. Phys.* **168**, 375 (1992).
 [13] K. Z. Xu, Z. P. Zhong, R. F. Feng, X. J. Zhang, L. F. Zhu, and X. J. Liu, *J. Electron Spectrosc. Relat. Phenom.* **94**, 127 (1998).
 [14] J. Geiger and H. Schmoranzler, *J. Mol. Spectrosc.* **32**, 39 (1969).
 [15] W. Fabian and B. R. Lewis, *J. Quant. Spectrosc. Radiat. Transf.* **14**, 523 (1974).
 [16] A. C. Allison and A. Dalgarno, *At. Data* **1**, 289 (1970).
 [17] A. C. Allison and A. Dalgarno, *Mol. Phys.* **19**, 567 (1970).
 [18] J. W. Liu and S. Hagstrom, *Phys. Rev. A* **48**, 166 (1993).
 [19] I. Borges and C. E. Bielschowsky, *Phys. Rev. A* **60**, 1226 (1999).
 [20] J. Berkowitz, *Atomic and Molecular Photoabsorption: Absolute Total Cross Sections* (Academic, San Diego, 2002).
 [21] M. Kitajima, S. Watanabe, H. Tanaka, M. Takekawa, M. Kimura, and Y. Itikawa, *J. Phys. B* **34**, 1929 (2001).
 [22] J. C. Nickel, P. W. Zetner, G. Shen, and S. Trajmar, *J. Phys. E* **22**, 730 (1989).
 [23] D. V. Fursa and I. Bray, *Phys. Rev. A* **52**, 1279 (1995).
 [24] S. Trajmar, J. M. Ratliff, G. Csanak, and D. C. Cartwright, *Z. Phys. D: At., Mol. Clusters* **22**, 457 (1992).
 [25] H. Kato, H. Kawahara, M. Hoshino, H. Tanaka, M. J. Brunger, and Y.-K. Kim, *J. Chem. Phys.* **126**, 064307 (2007).
 [26] L. Campbell, M. J. Brunger, P. J. O. Teubner, B. Mojarrabi, and D. C. Cartwright, *Aust. J. Phys.* **50**, 525 (1997).
 [27] <http://www-amdis.iaea.org/data/INDC-457/>
 [28] L. Vriens, *Phys. Rev.* **160**, 100 (1967).
 [29] E. N. Lassettre, *J. Chem. Phys.* **43**, 4479 (1965).
 [30] A. R. P. Rau and U. Fano, *Phys. Rev.* **162**, 68 (1967).
 [31] B. H. Bransden and C. J. Joachain, *Physics of Atoms and Molecules* (Longman, London, 1983).
 [32] M. J. Brunger, S. J. Buckman, and M. T. Elford, in *Photon and Electron Interactions with Atoms, Molecules and Ions*, edited by Y. Itikawa (Springer, Berlin, 2003), pp. 6-125 and 6-128.
 [33] P. A. Thorn *et al.*, *J. Chem. Phys.* **126**, 064306 (2007).
 [34] H. Kawahara, H. Kato, M. Hoshino, H. Tanaka, and M. J. Brunger, *Phys. Rev. A* **77**, 012713 (2008).
 [35] H. Kawahara, H. Kato, M. Hoshino, H. Tanaka, L. Campbell, and M. J. Brunger, *J. Phys. B* **41**, 085203 (2008).